Stochastic Environmental Research and Risk Assessment 17 (2003) 175–190 © Springer-Verlag 2003
DOI 10.1007/s00477-003-0132-x

Soil behaviour under dynamic loading conditions: experimental procedures and statistical trends

G. Christakos

Abstract. Soil behaviour under dynamic conditions is a crucial component of several studies concerned with the environmental effects of earthquakes, risk assessment and geological hazards. This work presents experimental procedures for studying soil behaviour under repeated loading and examines the role of uncertain parameters in the expected soil performance. Laboratory techniques are used to obtain stress controlled cyclic triaxial soil measurements, and a series of test programs are performed in order to study general statistical trends in the response of soils under simulated earthquake conditions, to investigate the processes causing soil failure, and to examine factors that may influence the results obtained in the laboratory.

Keywords: Cyclic soil testing, Dynamic loading, Liquefaction, Earthquakes

Introduction

There is a wide variety of environmental situations in which soils are subjected to repeated loading under essentially undrained conditions. Some of the sources of repeated dynamic loading with considerable environmental and ecological effects include, seismic loading during earthquakes, machinery vibrating at relative high frequencies, and traffic loading (Das, 1992; Jeffries and Been, 2002). Environmental scientists and soil engineers have studied problems such as the stability of soil deposits, earthquake-resistant design of earthworks, construction of safe offshore structures, ecological risk assessment and other situations where the soil was subjected to repeated loading. In order to evaluate the stability of soil deposits subjected to dynamic loading, information is required on the following features of soil performance (Christakos, 2003): the development of permanent irrecoverable strains and pore pressures with number of cycles; the variation of cyclic recoverable strains and pore pressures with number of cycles, including variation of soil modulus with number of cycles; the energy dissipation or

G. Christakos
Center for the Advanced Study of the Environment,
University of North Carolina at Chapel Hill, U.S.A.
and National Technical University of Athens,
Attiki, Greece
e-mail: george_christakos@unc.edu

This work has been supported by grants from the National Institute of Environmental Health Sciences (Grant no. P42-ES05948 and P30-ES10126) and the Army Research Office (DAAG55-98-1-0289).

damping behaviour of the soil; and the effect of repeating loading on the shear strength, dynamic strength (or liquefaction potential) of the soil. Considering the effects of repeated loading, two problems can be distinguished (Prakash, 1981; Kramer, 1995): (i) the short-term, undrained problem of soil behaviour (e.g., during an earthquake or individual storm); and (ii) the long-term, drained problem of soil behaviour (e.g., calm period during which drainage can take place and pore pressures equalize). However, problem (ii) is not studied for sands, as it does not have any significant effect on soil behaviour under cyclic loading.

Confronted with the problem of estimating the soil behaviour under repeated loading, a program of laboratory testing can follow two approaches: (a) Using the simple shear apparatus, where a horizontal shear stress can be applied to the sample which will deform under conditions of a simple shear state of strain such that the directions of the principal axes rotate during the test (Bjerrum and Landra, 1966; Finn et al., 1971; Prakash and Dakoulas, 1994). This type of test is relevant particularly for soil elements beneath a large gravity platform subjected to considerable wave forces. (b) Using the triaxial apparatus, which maintains fixed directions of principal axes, but always keeps two of the principal stresses equal (Silver, 1976; Das, 1992). Tests with fixed directions of principal axes in a plane strain apparatus are useful in providing clues as to how the triaxial results should be interpretated (since field loading is often approximated to conditions of plane strain than to axial symmetry). Some other apparatuses have been also used for studying the repeated loading behaviour of soils (Kramer, 1995), but their description is out of the purposes of this work.

In view of the above considerations, the aim of this work is twofold: (1) to suggest undrained stress-controlled cyclic triaxial test procedures to represent earthquake conditions and obtain the necessary measurements; and (2) to carry out testing programs in order to establish general statistical trends in the response of saturated sands to undrained stress-controlled cyclic loading conditions and, also, to investigate the cyclic stress conditions causing failure (mainly initial liquefaction) of sands. To achieve the above goals, the MAND-70 servo-hydraulic material testing machine has been used. The machine was found to be best suited for performing reasonably fast tests with low cost compared to other apparatuses while, at the same time, it permits better control of stresses and volume changes. Moreover, using this equipment one has simultaneous recording of load, deformations and pore pressures, while ensuring the maintainance of suitable load application, signal excitation, conditioning and recording equipment.

II
Theoretical description of cyclic triaxial soil testing

Soil dynamics relies on a group of techniques which base their concepts and models on measurements; these concepts and models lead, in turn, to mathematical formulations. The idealized cyclic loading conditions of a soil element in the field during an earthquake distinguish two stages as shown in the lower part of Fig. 1a (σ'_{v0} and σ'_{h0} are effective stresses and the τ is shear strength; Seed and Lee, 1966; Jeffries and Been, 2002). These field conditions may be simulated for a soil sample in the laboratory as in Fig. 1b using triaxial isotropically consolidated undrained tests with cyclic deviator stress applications (as usual, symbols without primes denote total stresses, whereas symbols with primes denote effective stresses). I.e., by the cyclic triaxial testing, generally speaking, cylindrical samples of soil are subjected to an axisymmetric system of stresses, particularly an iso-

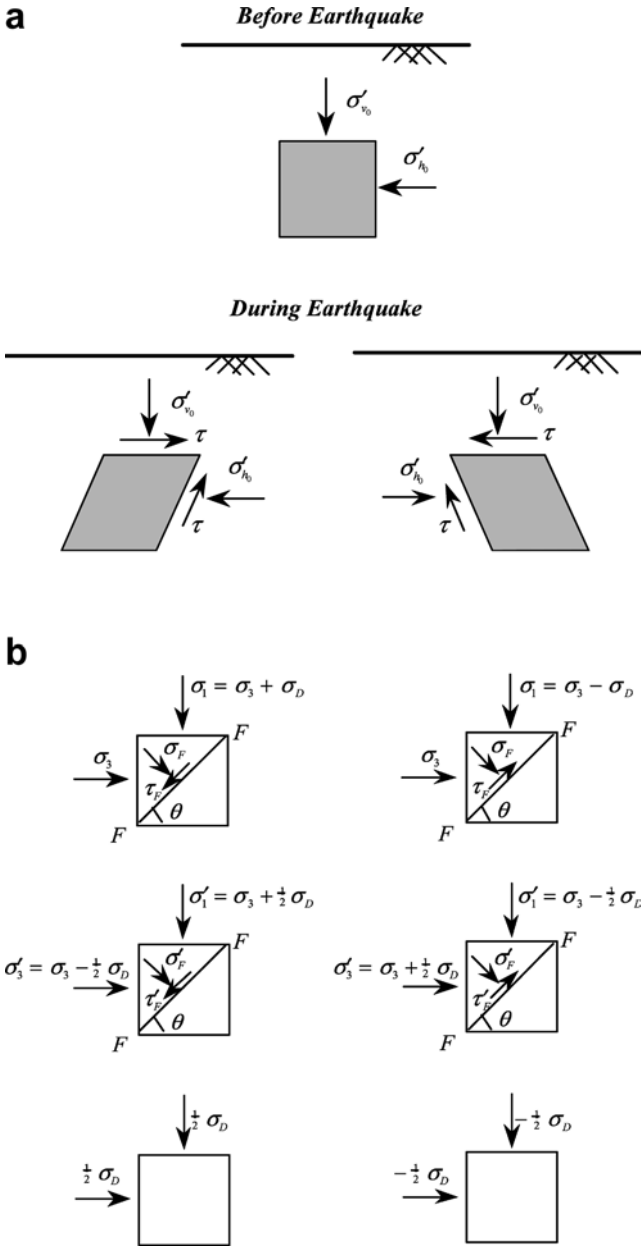

Fig. 1. **a** Idealized cyclic loading conditions of a soil element in the field during an earthquake. **b** Simulated cyclic loading conditions of a soil sample in the laboratory (symbols without primes denote total stresses, whereas symbols with primes denote effective stresses)

tropic stress σ_3 and an axial stress σ_1 that varies corresponding to a constant amplitude cyclic axial load. No drainage is allowed during the tests since the rise of pore pressure which reduces the effective stresses between soil particles is most critical when loading takes place before pore water has time to drain away. The

normal and shear stresses σ_F and τ_F, respectively, on the failure plane F-F are also depicted in Fig. 1b. In particular: (i) for the 1st stage (right side of Fig. 1b), $\sigma_F = \sigma_3 + \frac{1}{2}\sigma_D$, $\tau_F = \sigma_D$, and $\sigma'_F = \sigma_3$, $\tau'_F = \sigma_D$; (ii) for the 2nd stage (left side of Fig. 1b), $\sigma_F = \sigma_3 - \frac{1}{2}\sigma_D$, $\tau_F = -\frac{1}{2}\sigma_D$, and $\sigma'_F = \sigma_3$, $\tau'_F = -\frac{1}{2}\sigma_D$. Thus, the shear and the effective stresses on a plane making at 45° angle with the axis of the sample is expected to simulate the stresses acting on a horizontal plane in a soil element below a horizontal ground surface during an earthquake (no initial shear stresses acting before cyclic loading begins). The above conditions, which are developed by earthquake ground motions on soil elements below a level ground surface, could be simulated approximately in the laboratory by isotropically-consolidated undrained tests with cyclic deviator stress applications.

There are three main types of cyclic loading configurations with respect to the shear stress variations induced by variations in axial stress and overall pressure (Fig. 2): the one-way loading (no reversal of shear stress directions), the two-way loading with constant cell pressure (reversal of shear stress directions), and the two-way loading with variable cell pressure. The axial cyclic stress is wave-formed, which may assume one of the forms shown in Fig. 3. Among them, the sine wave-form is the most widely used, while the square one seems to lead to larger deformations and pore pressures (Christakos, 1980). Haversine and haversquare wave-forms apply only compressive loads resulting to one-way loading as above. On the other hand, a saturated sand subjected to cyclic loading is considered to reach the state of failure due to the phenomenon of liquefaction, when after a number of cycles it loses a large percentage of its shear resistance and flows in a manner resembling a liquid until the shear stresses acting on the soil mass are as low as its reduced shear resistance (Casagrande, 1971; Castro and Poulos, 1977; Cakmak, 1987). Before complete failure, the soil may experience some preliminary stages of liquefaction like, initial liquefaction (the state when a soil exhibits any degree of what might be considered to be liquefaction, but without failing), or partial liquefaction (no

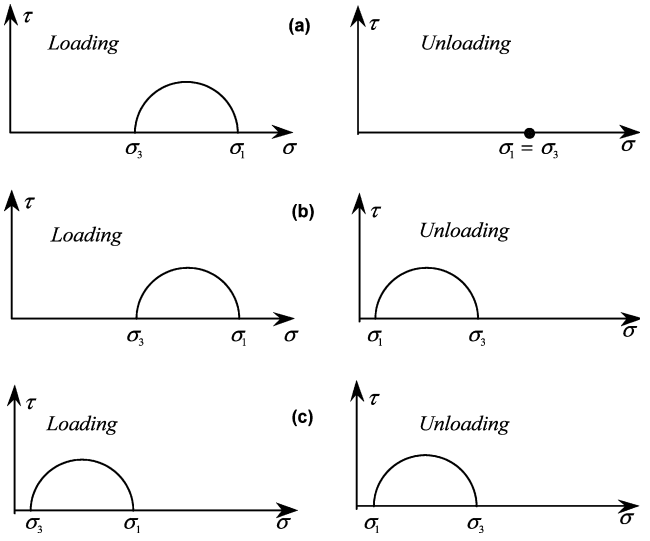

Fig. 2. Cyclic triaxial loading configurations; **a** one-way loading, **b** two-way loading with constant cell pressure, **c** two-way loading with varying cell pressure

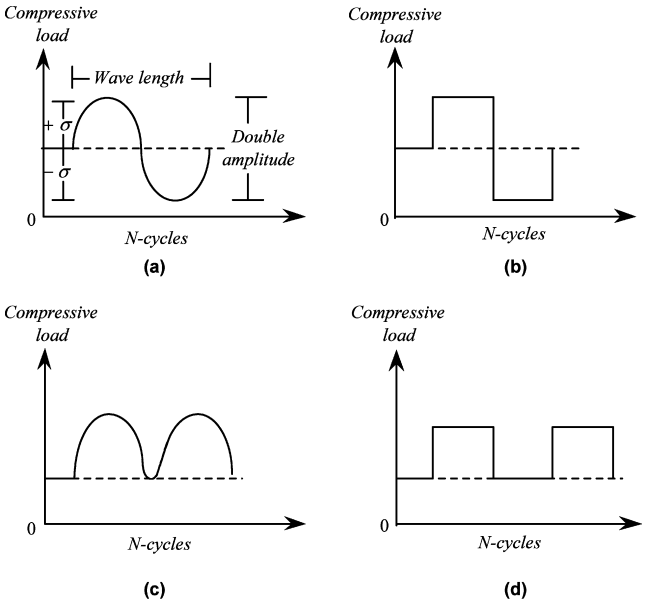

Fig. 3 a–d. Loading wave-forms. **a** Sine, **b** square, **c** haversine, and **d** haversquare wave-forms

resistance to deformation over a strain range less than that assumed to constitute failure). Furthermore, in simulated laboratorty experiments as well as in field situations the soil behaviour is characterized by considerable uncertainty, which implies that the relevant experimental variables are often modelled in terms of stochastic processes or random fields across space and time (Christakos, 1985, 1987, 1992). Hence, a statistical analysis of the experimental outcomes may be useful.

III
Parameters affecting soil behaviour during cyclic loading

Knowledge of the number of cycles required for liquefaction is only part of the solution for the behaviour of saturated sands. It has long been established that, prediction of ground motions, dynamic responses etc. requires knowledge of effective confining pressure, shear modulus and damping (Prakash, 1981; Prakash and Dakoulas, 1994). From a detailed study of the phenomenon (D'Appolonia, 1970; Kramer, 1995; Christakos, 2003), it became apparent that several parameters may affect the behaviour of saturated sands (stress-deformation, pore pressures, liquefaction, etc.) during cyclic loading. Within the context of this presentation, we have taken into account the most important of these parameters, namely:

(1) the frequency of loading (most authors recommend frequencies in the range 0.5–1.0 Hz);
(2) the failure criterion (as we saw above, one may consider several failure criteria like, initial, partial or complete liquefaction);
(3) the shape of wave-form of loading (as we saw above, there are several wave-forms currently in use by the various laboratories);
(4) the confining pressure (which can have a direct effect on pore pressures and the liquefaction process);

(5) the type of sand and certain of its properties (like, void ratio, or state of disturbance);
(6) the permanent and cyclic stress levels (the former is usually applied permitting drainage, whereas the latter is directly related to the number of cycles required to induce liquefaction).

The ideal cyclic loading test sample, would deform perfectly uniform, develop no non-uniformities of pore pressure, and should be tested in an apparatus equipped with a pore pressure measuring device with infinitely fast response, so that it could follow precisely the changes occuring in each cycle. In the discussion of the experimental programs in the following sections we examine how the above parameters may influence the cyclic behqviour of some sands.

IV
Equipment description

A brief description of the main parts of the MAND-70 servohydraulic dynamic testing machine employed in our experimental studies is as follows (Fig. 4):

Triaxial test cell and piston load

A triaxial cell suitable for cyclic test use is shown in Figs. 4 and 5 (this cell is similar, if somewhat larger, to standard cells). The sample is enclosed in a rubber membrane and sits in a cell that can be filled with air or water under pressure to provide an isotropic stress σ_3 on the soil. An axial stress σ_1 varies corresponding to a constant amplitude cyclic piston load. Hence, if the rum is pushed down ($\sigma_1 < \sigma_3$) while $\sigma_3 = \text{const.}$, we are in the state of one-way loading (compression, see Fig. 2a). If the rum is first pushed down ($\sigma_1 < \sigma_3$) while $\sigma_3 = \text{const.}$, we have a two-way loading with constant cell pressure (compression-extension, reversal of shear directions, Fig. 2b). Finally, it is possible that the cell pressure and the cyclic axial stress vary simultaneously, with or without a phase difference (two-way loading with variable cell pressure, Fig. 2c). In the test programs carried out for the purposes of this presentation, air has been used as the cell fluid. No drainage is allowed during the tests since, as we will see later, the rise of the pore pressure which reduces the effective stresses between soil particles, is most critical when loading takes place before pore water has time to drain away.

Control console

This is an electronic equipment capable to ensure the application onto the soil sample the combination of loading characteristics which we decide to be appropriate for each test (frequency, wave-form, amplitude of cyclic load, etc.). A detailed layout is given in Fig. 5.

Recorder and measuring units

Using the recorder-unit of Fig. 6 we achieved the simultaneous recording of load, deformation, and pore pressures. During the tests both axial deformation and axial load have been measured using the loading pistons indicated (Figs. 4), or the deformation measuring equipment that consists of linear variable differential transformers (LVDT) attached to the soil sample by a pair of clamps (Fig. 4b). We need two LVDT to measure axial deformations. Pore pressures have been recorded using a pore pressure transducer (10 Kgf).

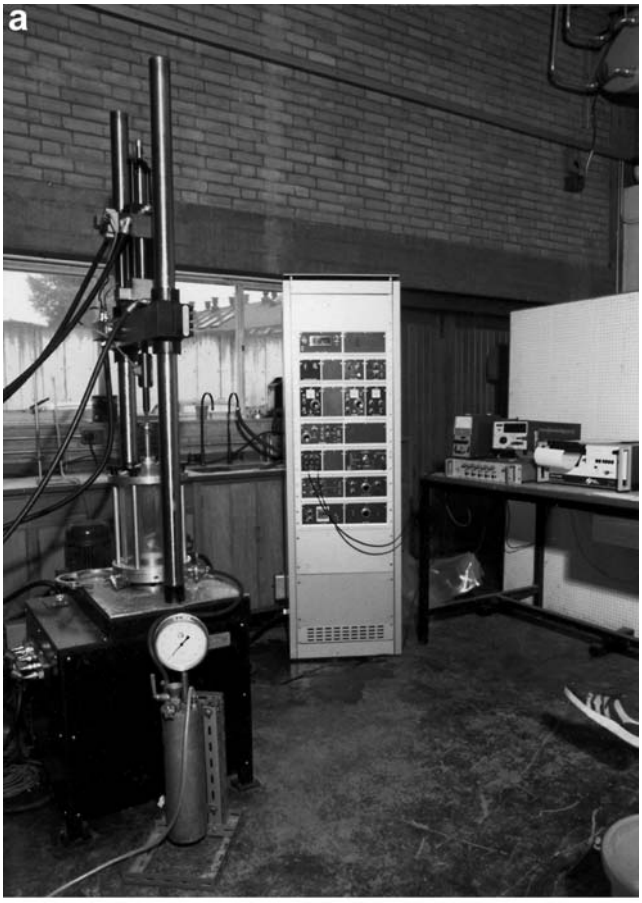

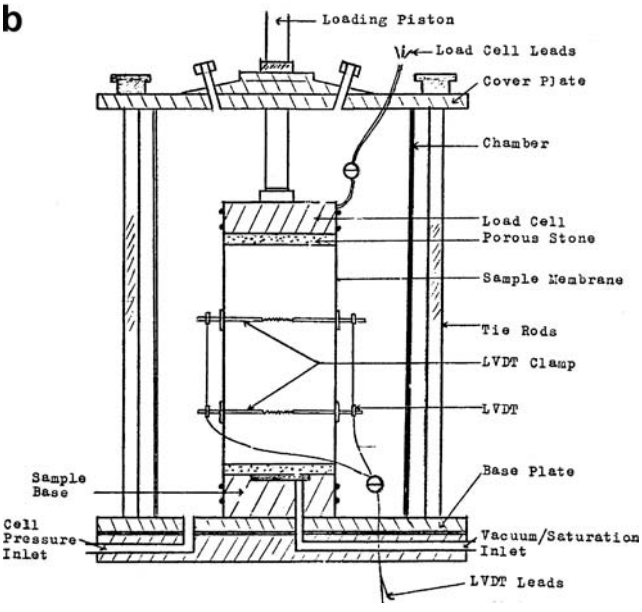

Fig. 4. **a** MAND-70 dynamic soil testing apparatus. **b** Triaxial test cell

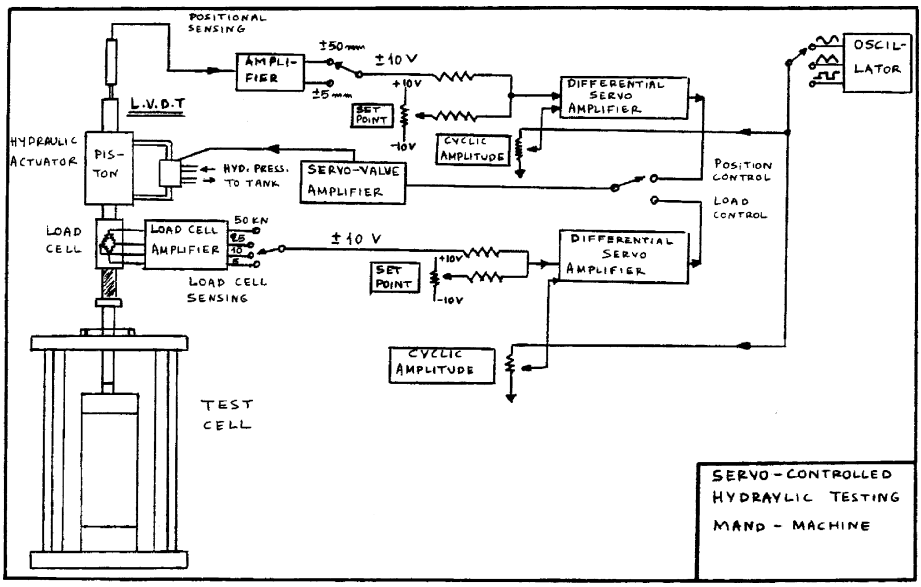

Fig. 5. Layout of the dynamic loading equipment

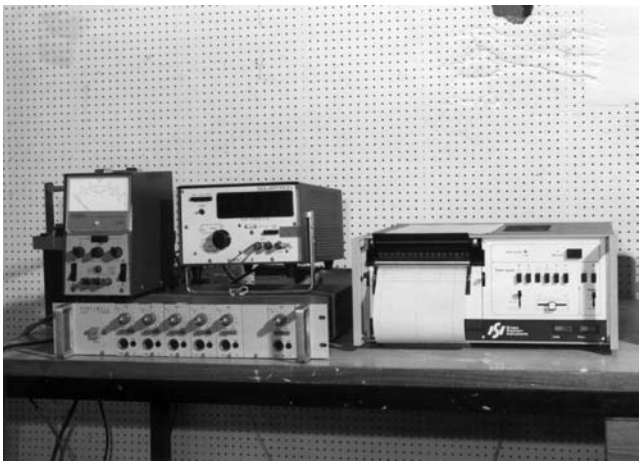

Fig. 6. Recorder and measuring units

Additional equipment

This includes tools like, compressed air source and regulator, vacuum source and bubble chamber, compaction apparatus, calibrators, membrane stretcher, porous stones etc.

V

Testing procedure

A step-by-step standardized cyclic triaxial test procedure for the evaluation of the dynamic features of soils is not generally available (this is mainly due to the diversity of cyclic triaxial equipment currently in use, etc.). The proposed test

equipment and testing procedure have been shown to be significant, in the sense that they met the standards required for dynamic soil testing and, also, the results of tests on a standard soil sample agreed with well-established values obtained by other laboratories. Certainly, both the test equipment and testing procedure have been open to further improvement. The testing procedure and material reported herein are summarized as follows:

Step 1 (Soil description)
In this stage the sand used is analyzed and classified (grain size distribution, specific gravity, maximum and minimum porosities, maximum and minimum dry densities etc.). Two types of sands have been used (Table 1b and Fig. 7): Sand No. 1, which is Leighton Buzzard, a medium to coarse sand; and Sand No. 2, which is a fine to medium sand (this sand type has been selected because liquefaction occurs most likely in fine to medium sands and, thus, more representative results may be obtained).

Step 2 (Sample preparation)
Samples 100 mm in diameter and 200 mm high can be accommodated in the triaxial cell shown in Fig. 4b. This size is especially recommended for resilient modulus testing, but other combinations of ratios length over diameter could be used (sample length should not be less than twice the diameter). Some changes in sample densities could happen during penetration or during testing when drainage has taken place. Each sample has been compacted in layers in a rubber membrane confined by a split mould attached to the bottom pedestal of the triaxial cell. In order to obtain a uniform density, the bottom layers had to be slightly undercompacted, since compaction of each succeeding layer densifies the sand in layers below it. The top cap was tapped until the desired dry density was obtained. Next, the test sample was saturated applying a back pressure of about 70–80 psi or more, while permitting drainage from the top cap. The final back pressure value is determined by increasing the back pressure until the B-facotr (ratio of the change in pore pressure to change in cell pressure) did not increase with an additional increase in back pressure. Before applying back pressure, we

Table 1. Sample Description

(a) Sand No. 1: Leighton Buzzard.
- Grain size distribution: See Fig. 7a. Medium to coarse sand (70% medium and 30% coarse).
- Specific gravity: $G_S = 2.65$.
- Max. and min. porosities: $n_{max} = 44\%$, $n_{min} = 35\%$.
- Max. and min. dry densities: $\nu_{d,max} = 1.69$ gr/cm^3, $\nu_{d,min} = 1.45$ gr/cm^3.
- Dry density of samples used: $\nu_d = 1.57$ gr/cm^3
- Void ratio of samples used: e = 0.64.
- Relative density of samples used: $D_r = 60\%$

(b) Sand No. 2: A mixture of several sands (Biddulph, Redhill, etc.).
- Grain size distribution: See Fig. 7b. Fine to medium sand (~6% fine and 90% medium).
- Specific gravity: $G_S = 2.65$.
- Max. and min. porosities: $n_{max} = 45.95\%$, $n_{min} = 35.5\%$.
- Max. and min. dry densities: $\nu_{d,max} = 1.68$ gr/cm^3, $\nu_{d,min} = 1.41$ gr/cm^3.
- Dry density of samples used: $\nu_d = 1.58$ gr/cm^3
- Void ratio of samples used: e = 0.67
- Relative density of samples used: $D_r = 60\%$.

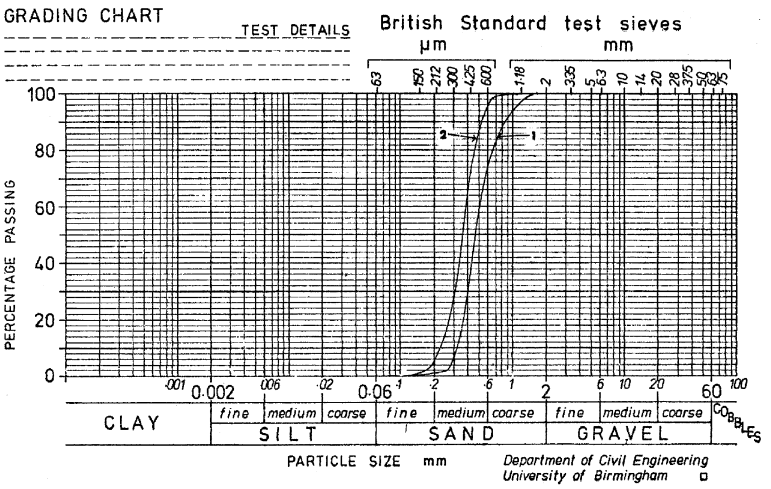

Fig. 7. Grain size distribution of **a** Sand No. 1, and **b** Sand No. 2

may flush through with CO_2 to dissolve air, permitting drainage (that requires approximately 30–35 psi for 10–20 minutes). Note that during saturation, a constant effective confining pressure is required to minimize the unrecorded volume changes. After completion of saturation, the sample is consolidated to the final required effective stress. During this phase of the test, changes in volume and axial height may be recorded (this allows calculations to be made of the relative density of the sample after consolidation and prior to cyclic loading, see below).

Step 3 (Cyclic loading)
The sample is loaded without drainage using a servo-hydraulic loading system (Fig. 4a). Depending on the programmed test, one may adjust the switches of the control console on the proper positions. E.g., if we intend to carry out a triaxial strength test we have to decide the frequency, the wave-form, the constant cell pressure, and the constant amplitude cyclic load applied during the programmed test.

Step 4 (Results)
The results were recorded on a special Kodak-1895 paper using Ultra Violet recorder under scale. A statistical analysis of the results then followed to identify trends in the soil behaviour under dynamic loading.

VI
Test programs

The specified experimental programs carried out had three main purposes: (a) to qualify the use of the MAND-70 testing equipment within the limits of cyclic soil performance; (b) to establish some general statistical trends on the behaviour of sands under cyclic loading; and (c) to conduct a series of tests to failure. The test programs are as follows:

Test Program No. 1
During this program a series of tests were performed. Each sample was subjected to a complex and irregular loading sequence, while several observations related to cell pressure, axial cyclic load, frequency, wave-form, axial deformation, pore

pressure etc. were made. Each stage of the test included 30 cycles, while between each stage the sample was drained to allow excess pore pressures to dissipate. Results of this program are presented in Figs. 8–12, in which the statistical means for a series of tests are plotted etc..

Test Program No. 2

A number of tests to failure – each with a single set of loading conditions – are conducted. Results are given in Figs. 13–15. In Fig. 13a the sample distortion at point of liquefaction due to pore pressure non-uniformities is shown. In Fig. 13b a typical liquefied sample is shown.

Discussion of the results (Figs. 8–15) for both test programs is given in the following section. Note that, when carrying out these tests one assumption made was that there were negligible changes in density and shear strength when

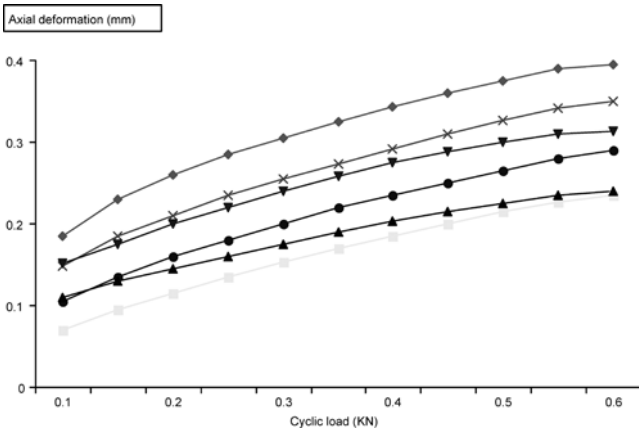

Fig. 8. Statistical trend of axial deformation vs. cyclic load of sine wave-form (×, ●, ■) and square wave-form (◆,▼,▲); $\sigma_{3c} = 100$ KN/m^2 The ν is the loading frequency (Hz): $\nu = 0.5$ (◆, ×), = 1.0 (▼, ●); = 1.5 (Δ, ■)

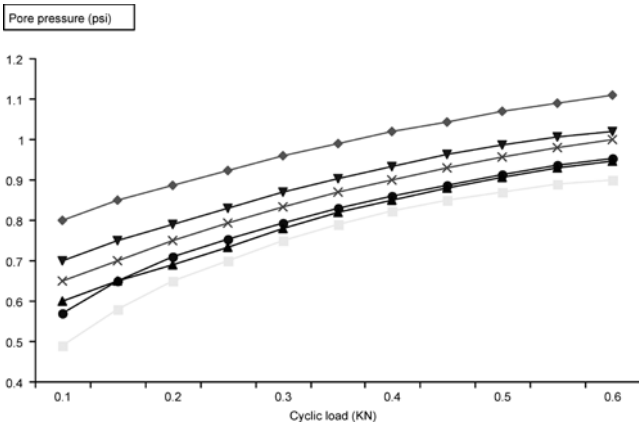

Fig. 9. Statistical trend of pore pressure vs. cyclic load of sine wave-form (×, ●, ■) and square wave-form (◆, ▼, Δ); $\sigma_{3c} = 100$ KN/m^2. The ν is the loading frequency, in Hz: $\nu = 0.5$ (◆, ×), = 1.0 (▼, ●); = 1.5 (Δ, ■)

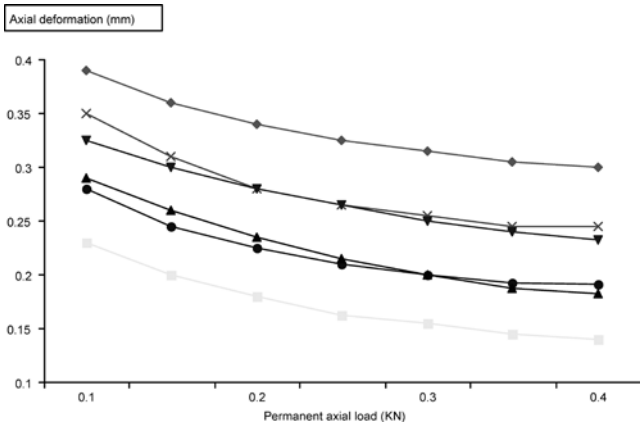

Fig. 10. Statistical trend of axial deformation vs. permanent load for sine wave-form (×, ●, ■) and square cyclic wave-form (◆, ▼, ▲). The ν is the loading frequency, in Hz: $\nu = 0.5$ (◆, ×), $= 1.0$ (▲, ●); $= 1.5$ (▲, ■)

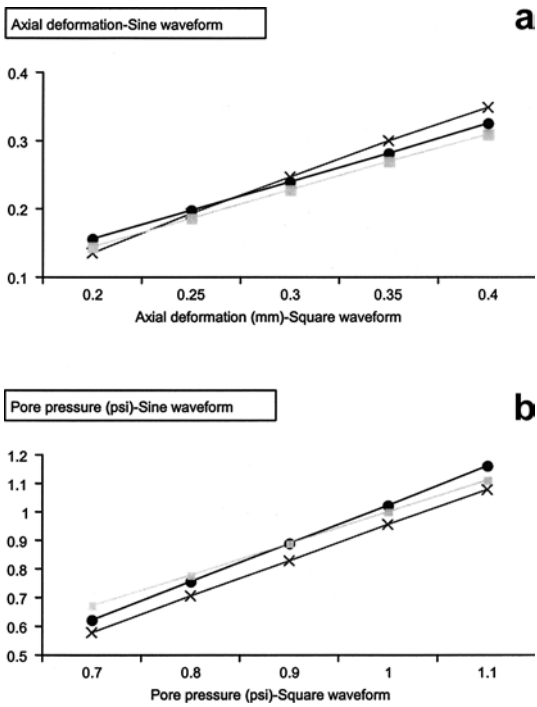

Fig. 11. Statistical trend of **a** axial deformation and **b** pore pressure (sine wave-form vs. square wave-form). The ν is the loading frequency, in Hz: $\nu = 0.5$ (×), $= 1.0$ (●), $= 1.5$ (■)

preparing the samples or during testing them. Certain experimental issues that arose during the Test Programs No. 1 and 2 carried out in this work are worth-mentioning. These issues were related to the following parameters:

(a) Pore pressures during tests

Difficulties arise in measuring permanent pore pressures, cyclic variations of pore pressures and, also, in interpretating whether the measured pressures are truly representative of the pore pressures in the whole sample. In our tets the measured

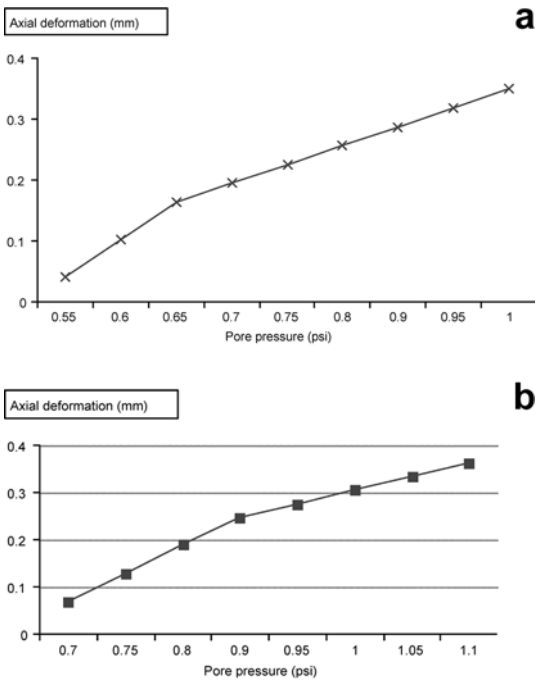

Fig. 12. Statistical trend of axial deformation vs. pore pressure: **a** sine wave-form, and **b** square wave-form ($\nu = 0.5$ Hz)

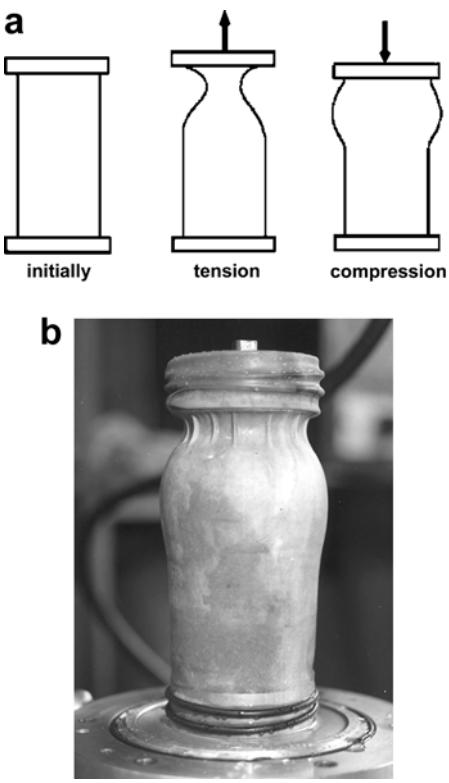

Fig. 13. **a** Distortion of samples during liquefaction due to non-uniformities of pore pressures; and **b** typical sample of sand failed to liquefaction. ($\nu = 0.5$ Hz)

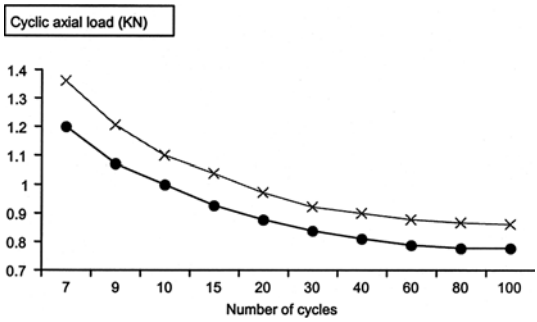

Fig. 14. Cyclic axial load vs. number of cycles to initial liquefaction for sine wave-form (×) and square wave-form (●). $\sigma_{3c} = 100$ KN/m^2 and $\nu = 1$ Hz

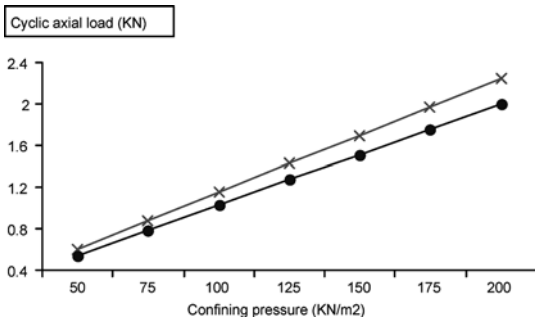

Fig. 15. Effect of confining pressure (σ_{3c}; in KN/m^2) on the cyclic axial load causing inital liquefaction for sine wave-form (×) and square wave-form (●)

pore pressure variations were, on the average, less than expected (presumably because of the difficulties associated with measurement). The permanent pore pressures have been observed to keep on increasing some time after the last cycle has been applied (this could be an explanation of some earth movements observed some days after the end of an earthquake). Cyclic pore pressure measurements via the side drain have been found to be statistically more accurate than those obtained via the end of the sample. More specifically, cyclic pore pressure measurements via the sides of the sample may be up to 20% below the value in the soil, when via the end platens are between 30–40% low. The statistical analysis of the experimental results demonstrated that more accurate pore pressure measurements are obtained when using sine wave-form than by using square wave-form. Regarding the measuring system, it must respond fast enough to follow cyclic variations at the agreed test frequency. To ensure high degrees of saturation in the sample and pore pressure measuring systems, careful deairing and the use of a fairly high back pressure are necessary.

(b) Friction on piston

This is an issue that has been handled in the particular project by using grease and a special PTFA spray that reduce the friction. A better way might be to measure the axial load inside triaxial cell, so no correction for friction will be required.

(c) Drainage system

The easiest way to measure the flow of water from the sample during the consolidation stage is by using byrettes. However, volume changes may be more accurately computed from the measurements of axial deformations during consolidation. In this case we made the assumption that isotropic consolidation

produced isotropic deformations, whereas anisotropic consolidation produced purely one-dimensional deformations.

Shape of the load pulse
This is a rather important issue related to the loading equipment used. In this work the issue has been resolved by the appropriate adjustement of the Loop Gain on the control console.

VII
Discussion

Insight is provided into certain aspects of soil behavior under repeated loading by means of experimental investigation and statistical analysis. The analysis of the experimental results of the Test Program No. 1 summarized in Figs. 8–12 indicates that the axial deformations and the pore pressures for the square-wave loading increase, on the average, more rapidly than for the sine-wave loading (resulting, of course, in lower cyclic strength values). The average curves obtained from the same experimental results (Figs. 8 and 9) have shown that a lower loading frequency resulted in larger and more rapid axial deformations and pore pressures. Also, higher confining pressures may result in much slower increase in pore pressures. In Fig. 10 one can see the mean variations in maximum double amplitude axial deformation vs. permanent axial load for sine wave-form and square wave-form, respectively. So, when the permanent load is increasing the max.d.a. axial deformation is reducing; the same happens with the pore pressures. That is because increasing the permanent load resulted in consolidation of the sample. A decrease in the rate of strain is as well observed, whereas increasing the frequency of loading leads to a reduction of the max.d.a. axial deformation. The mean variations of axial deformations, sine wave-form vs. square wave-form, and pore pressures, sine vs. square wave-form, are rather linear (Fig. 11). The same happens with the mean variation of axial deformations (double amplitude) vs. pore pressures, Fig. 12, so that, generally speaking, we could say that the pore pressures variation rather follows the axial deformation trends.

In the tests performed during Test Program No. 2 it was found that cyclic triaxial strength is related to the sample preparation procedures, the small changes in sample dry density, the shape of the cyclic load trace, the confining pressure, the void ratio and the failure criterion. Results shown in Figs. 13–15 indicate that samples tested using a square-wave loading, show strength values which statistically are 10–20% less than those obtained using a sine-wave loading. The use of a sine wave-form is much more recommended when representing earthquake ground motions on soil below level ground than the use of square wave-form (very severe square wave-form must be avoided). The undrained shear strength, pore pressure and deformation at failure are rather not influenced by sample geometry and end conditions. The higher the cyclic stress or strain to which the sample is subjected, the smaller is the number of load cycles required to induce liquefaction (Fig. 14). Moreover, the higher the confining pressure acting on the sample, the higher the cyclic loads (Fig. 15) deformations, or number of cycles required to induce liquefaction. If a loose sample liquefies under constant amplitude cyclic stresses, then very large deformations will be observed. In summary, liquefaction is expected to occur in samples that are highly contractive, i.e., their state of stress and density must be as such as to lie above the steady-state line in the state diagram (most likely it happens in uniform fine, clean loose sand; Castro and Poulos, 1977; Cakmak, 1987). It is noteworthy that static loads

can cause liquefaction. Cyclic load causing shear stresses larger than the steady-state strength also can cause liquefaction.

Long term changes in pore pressure during both test programs (complex and irregular cyclic loading and undrained dynamic strength testing) are reliable because time of equalization occurs and the measuring system has acceptably low compliance. Furthermore, small differences in the operation of the apparatus – errors in the shape of the loading trace etc – were found to cause significant errors. Another source of errors is the compliance arising from changes in membrane penetration into peripheral voids as the pore water pressure increases. It was observed that tensile forces applied on the sample cause greater axial deformations than compressive forces. Hence, the double amplitude deformation from two-way loading was more than twice that from one-way loading. Last but not least, it is confirmed that sample preparation techniques are more critical than were expected to be, while at present time we cannot recommend a particular laboratory sample preparation technique which best models the field performance of soils. Concluding this work, we emphasize that it is through better understanding of the fundamentals of soil science that further improvements in experimentation can be made.

References

Bjerrum L, Landra A (1966) Direct simple shear tests on a Norwegian quick clay. Geotechnique 26(1): 1–20

Cakmak AS ed. (1987) Soil Dynamics and Liquefaction. Developments in Geotechnical Engineering, No 42, Elsevier Science Ltd, NY

Casagrande A (1971) On liquefaction phenomenon. Geotechnique, XXI(3): 197–202

Castro G, Poulos SJ (1977) Factors affecting liquefaction and cyclic mobility. ASCE 103(GT6): 501–516

Christakos G (1980) Soil-structure interaction: A laboratory apparatus for studying the behavior of soils under dynamic loading. Research Report, Foundation Engineering, University of Birmingham, UK, pp. 248

Christakos G (1985) Modern statistical analysis and optimal estimation of geotechnical data. Engineering Geology, 22(2): 175–200

Christakos G (1987) A stochastic approach in modelling and estimating geotechnical data. Intern. Jour. of Numerical Analytical Methods in Geomechanics 11(1): 79–102

Christakos G (1992) Random Field Models in Earth Sciences. Academic Press, San Diego, CA

Christakos, G (2003) Experimental studies of soil behavior under seismic loading conditions. Research Report 1-03, Department of Mining and Metallurgical Engineering, National Technical University of Athens, Athens, Greece, pp. 39

D'Appolonia E (1970) Dynamic loadings. ASCE, 96(SM1): 49–72

Das BM (1992) Principles of Soil Dynamics. PWS Publishing Co., Boston, MA

Finn WDL, Pickering DJ, Bransby PL (1971) Sand liquefaction in triaxial and simple shear tests. ASCE, 97(SM4): 635–659

Jeffries M, Been K (2002) Soil Liquefaction. Taylor Francis, London, UK

Kramer SL (1995) Geotechnical Earthquake Engineering. Prentice Hall, Upper Saddle River, NJ

Prakash S (1981) Soil Dynamics. McGraw-Hill Co., New York, NY

Prakash S, Dakoulas P eds. (1994) Ground Failures Under Seismic Conditions. Geotechnical Engineering Division, American Society of Civil Engineers; Reston, VA

Seed HB, Lee KL (1966) Liquefaction of saturated sands during cyclic loading. ASCE, 92(SM6): 105–134

Silver ML (1976) Laboratory triaxial testing procedures to determine the cyclic strength of soils. Report No. NUREG-31, U.S. Nuclear Regulatory Commission, Washington DC